Cation disorder and the metal-insulator transition temperature in manganese oxide perovskites

Lide M. Rodriguez-Martinez and J. Paul Attfield
Department of Chemistry, University of Cambridge, Lensfield Road, Cambridge CB2 1EW, United Kingdom and Interdisciplinary Research Centre in Superconductivity, University of Cambridge, Madingley Road, Cambridge CB3 0HE, United Kingdom
(Received 24 March 1998)

Structural changes in a series of 30% hole-doped $A\mathrm{MnO_3}$ perovskites have been studied by powder neutron diffraction. Large local changes, consistent with the freezing of Jahn-Teller distortions of the $\mathrm{MnO_6}$ octahedra, occur at the metal-insulator transition at $T_m = 363$ K in $(\mathrm{La_{0.70}Ca_{0.11}Sr_{0.19}})\mathrm{MnO_3}$. The 4 K structures of four compositions with the same *A*-cation radius but increasing amounts of *A*-site disorder, show an increasing radial distortion of the $\mathrm{MnO_6}$ octahedra. The decrease in T_m across this series may reflect these increasing distortions which lower the local strain contribution to the transition enthalpy. [S0163-1829(98)05030-9]

A variety of electronic and magnetic states are observed in doped $A\mathrm{MnO_3}$ perovskites where the *A* sites are occupied by a mixture of trivalent lanthanide (L) and divalent Ca, Sr, or Ba (M) cations. The transition from a low-temperature ferromagnetic metallic state to a high-temperature paramagnetic insulating phase has been of particular interest as it gives rise to colossal negative magnetoresistances at the metal-insulator transition temperature T_m.[1,2]

We have previously shown[3] that in a series of $(L_{0.7}M_{0.3})\mathrm{MnO_3}$ perovskites with a constant mean *A*-site cation radius $\langle r_A \rangle$ T_m shows a strong linear dependence upon the variance (second moment) of the *A*-cation radius distribution $\sigma^2 = \langle r_A^2 \rangle - \langle r_A \rangle^2$.[4] For this series of samples with $\langle r_A \rangle = 1.23$ Å, the experimental value of $dT_m/d\sigma^2$ is $-20\,600 \pm 500$ K Å^{-2}. This effect was attributed to displacements of the oxygen atoms due to the *A* site disorder, as shown by the simple model in Fig. 1. This shows that σ provides a measure of the oxygen displacements Q due to *A* cation size disorder and that $(r_A^0 - \langle r_A \rangle)$ is the complementary measure of displacements due to $\langle r_A \rangle$ being less than the ideal value r_A^0. This is defined as giving a tolerance factor $t = 1$ [$t = (\langle r_A \rangle + r_\mathrm{O})/\sqrt{2}(r_\mathrm{Mn} + r_\mathrm{O})$; r_O and r_Mn are the radii of the oxide and manganese ions].

To investigate the structural changes in $A\mathrm{MnO_3}$ perovskites as a function of σ^2 and at the metal-insulator transition, four of the previously reported compositions[3] have been studied by time-of-flight (TOF) powder neutron diffraction at 4 K on the POLARIS diffractometer at the ISIS source, Rutherford-Appleton Laboratory, U.K. The four samples (Table I) have the same $x = 0.3$ doping level and $\langle r_A \rangle = 1.23$ Å, and show a linear decrease of T_m with σ^2. A variable temperature study of the sample with the smallest σ^2 $(\mathrm{La_{0.70}Ca_{0.11}Sr_{0.19}})\mathrm{MnO_3}$ was also carried out using a cryostat and furnace to access temperatures between 4 and 550 K.

TOF data from detector banks at $2\theta = 35°$ and 145° were Rietveld-fitted simultaneously[5] providing data down to 0.4 Å d spacings which enabled the atomic displacement factors to be refined accurately. The profiles for $(\mathrm{La_{0.70}Ca_{0.11}Sr_{0.19}})\mathrm{MnO_3}$ show that a transition from the high-temperature rhombohedral structure ($R\bar{3}c$ symmetry) to a low-temperature orthorhombic ($Pnma$) phase occurs below 200 K. Fits to the TOF data show that the two phases coexist in this region, as found elsewhere,[6] and at 4 K the sample consists of 82% orthorhombic and 18% rhombohedral phases. The 4 K patterns of the other three samples were fitted by the orthorhombic $Pnma$ structure and no evidence for a rhombohedral component was found. The combined R_{wp} residuals for the refinements were 1.5–1.6% and the reduced χ^2 values were between 2.9 and 3.7.

A structural discontinuity is observed in rhombohedral $(\mathrm{La_{0.70}Ca_{0.11}Sr_{0.19}})\mathrm{MnO_3}$ at T_m (Fig. 2), as found in many other manganites.[7–11] Although the average $\bar{3}$ crystallographic symmetry of the $\mathrm{MnO_6}$ octahedra is unchanged at the transition, small anomalies in the Mn-O bond distance and Mn-O-Mn angle are observed. To measure changes in local structure at T_m, the displacement parameter for the oxygen atom around the mean position was refined anisotropically for data between 150 and 550 K. The principal mean square displacements perpendicular to the Mn···Mn vectors u_2 and u_3 vary smoothly [Fig. 2(b)] whereas a clear discontinuity in the u_1 data at T_m shows that significant local changes in the

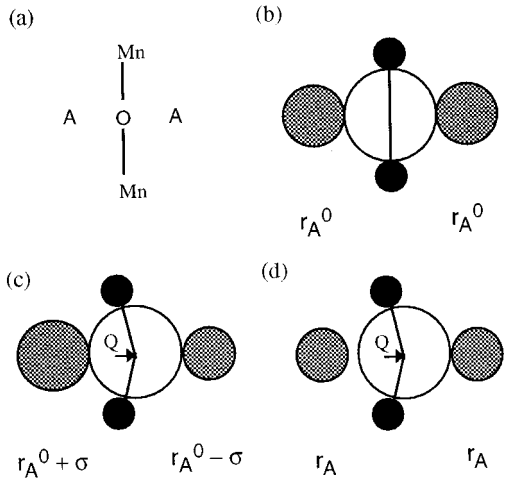

FIG. 1. Model for local oxygen displacements in $A\mathrm{MnO_3}$ perovskites. A fragment of ideal cubic structure with *A* cations of radii r_A^0 is shown schematically in (a) and as spherical ions in (b). Cation size disorder in (c) gives rise to random oxygen displacements $Q = \sigma$ and a reduction in the *A* site radius in (d) leads to ordered oxygen displacements $Q = r_A^0 - r_A$.

TABLE I. *A* site compositions and their σ^2 values, T_m's (Ref. 3), and selected parameters from the 4 K powder neutron refinements (cell parameters and volume, Mn and *A* site magnetic moments and Mn-O-Mn angles, with estimated standard deviations in parentheses).

A site composition	σ^2 (Å^2)	T_m (K)	a (Å)	b (Å)	c (Å)	V (Å^3)	$\mu_{Mn}(\mu_B)$	μ_A (μ_B)	Mn-O(1)-Mn (deg.)	Mn-O(2)-Mn (deg.)
$La_{0.70}Ca_{0.11}Sr_{0.19}$	0.0016	363	5.4586(1)	7.7146(2)	5.5005(1)	231.63(1)	3.55(1)	0	161.24(6)	165.29(4)
$La_{0.32}Pr_{0.38}Sr_{0.30}$	0.0029	336	5.4544(1)	7.7067(2)	5.4953(1)	231.00(1)	3.61(1)	0.14(2)	161.12(4)	164.27(3)
$Pr_{0.70}Sr_{0.23}Ba_{0.07}$	0.0074	247	5.4602(2)	7.7102(2)	5.4852(2)	230.92(2)	3.55(1)	0.29(1)	159.96(7)	162.72(5)
$Nd_{0.70}Sr_{0.16}Ba_{0.14}$	0.0123	146	5.4680(2)	7.7263(3)	5.4800(2)	231.52(1)	3.56(1)	0.37(2)	159.19(9)	162.14(6)

Mn-O bond lengths occur at the transition. This has previously been observed in the orthorhombic perovskite $La_{0.75}Ca_{0.25}MnO_3$.[7,8] By extrapolating the thermal variations of u_1 from above and below T_m to zero temperature, the increase due to static displacements is estimated to be $\Delta u_1 \approx 0.004$ Å^2, equivalent to a root mean square deviation of ± 0.06 Å about the mean Mn-O bond length of 1.96 Å. This is consistent with a change from dynamic Jahn-Teller distortions (mobile polarons) below T_m to static, disordered distortions (trapped Jahn-Teller polarons) above the transition.[8,9,12] Only 70% of the Mn sites contain Jahn-Teller distorted Mn^{3+} and the other 30% Mn^{4+} sites prevent the formation of a long-range cooperatively distorted structure such as that found in undoped $LaMnO_3$.[13] The enthalpy difference between the dynamic and static Jahn-Teller states at $T=0$ may be estimated as $\Delta H_S = 6K\Delta u_1/2$ per Mn atom (bonded to six oxygen atoms). Taking the force constant for the Mn-O bond to be $K \approx 100$ Nm^{-1} (Ref. 14) gives $\Delta H_S/k_B \approx 900$ K (k_B is the Boltzmann constant), which is a significant energy in comparison to $T_m = 363$ K.

The four 4 K $AMnO_3$ refinements (Table I) give the mean ferromagnetically ordered moments at the Mn site and the *A* site for samples containing magnetic lanthanides. The Mn moments are close to the ideal value of $3.7\mu_B$ and show no significant variation with σ^2, which rules out an increasing spin disorder as the cause of the decrease of T_m across the series. Although the cell parameters of these phases show a decreasing orthorhombicity with increasing *A* cation size variance σ^2, the local distortions of the MnO_6 octahedra increase with σ^2. This is evidenced both by the ordered orthorhombic distortion of the octahedra [Fig. 3(a)] and from the increasing oxygen atomic displacement factors [Figs. 3(b) and 3(c)]. The increasing dispersion in the three pairs of inequivalent Mn-O distances is reflected by a small increase in the average Mn-O distance and slight decreases in the

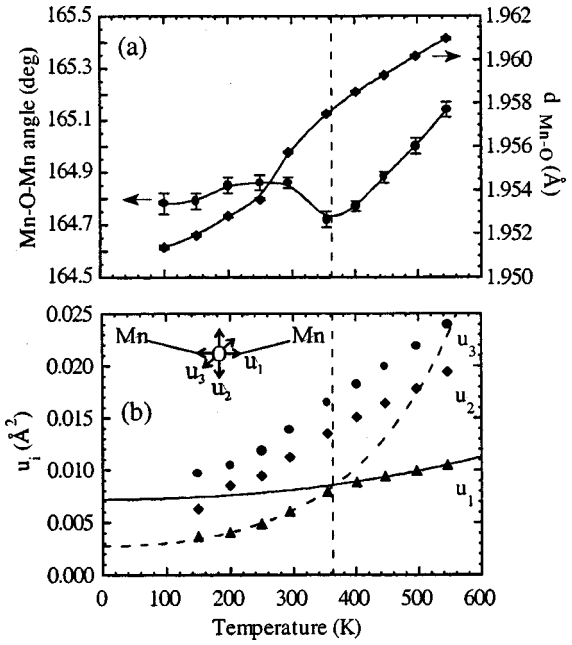

FIG. 2. Thermal variation of (a) mean Mn-O distance and Mn-O-Mn angles, and (b) mean squared oxygen displacements in the directions shown for rhombohedral $(La_{0.70}Ca_{0.11}Sr_{0.19})MnO_3$.

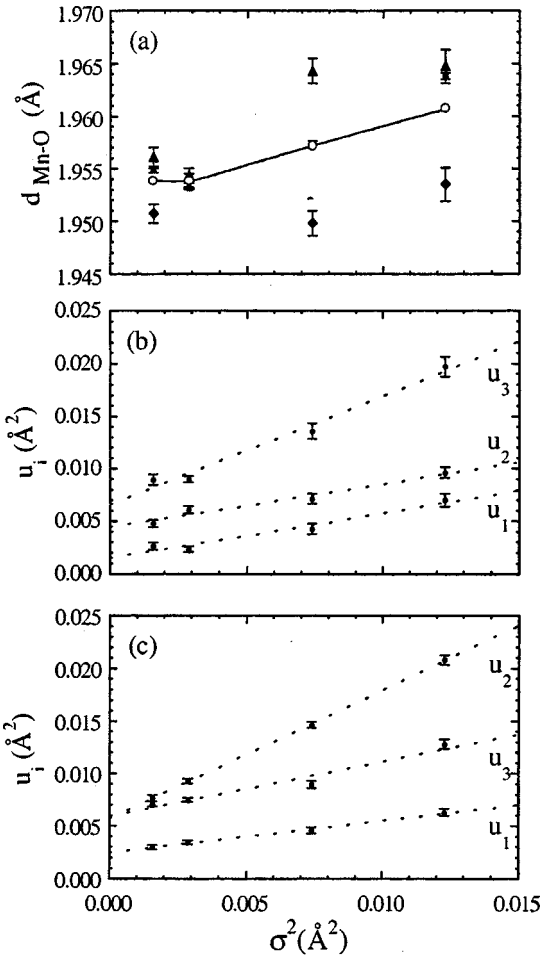

FIG. 3. Variation of the orthorhombic 4 K structures with *A*-site disorder; (a) Mn-O distances with the average shown as connected open points, and principal mean squared oxygen displacements in the directions shown in Fig. 2(b) for the crystallographically distinct O(1) site at (0.49, $\frac{1}{4}$, 0.05) (b) and O(2) at (0.27, 0.03, -0.27) (c).

Mn-O-Mn angles (Table I). Much larger changes in local structure with increasing σ^2 are evidenced by the u_i values in Fig. 3(b), which show an approximately linear increase with σ^2 due to increasing static disorder as the change in the phonon contribution at 4 K is minimal.

In the ideal $A\mathrm{MnO_3}$ perovskite structure, each O atom is coordinated octahedrally by four A and two Mn cations. The simple model in Fig. 1 shows that in an ideal cubic perovskite with mean A cation radius r_A^0, cation disorder only gives rise to oxygen displacements perpendicular to the Mn-O-Mn axis [i.e., $Q_1^2=0$ and $Q_2^2=Q_3^2=\sigma^2$, giving $\langle Q^2\rangle = 0.67\ \sigma^2$, with the displacement directions as shown in Fig. 2(b)]. The slopes $\Delta u_i/\sigma^2$ of the plots in Figs. 3(b) and 3(c) give experimental measurements of the dependences of Q_i^2 upon σ^2 in our series of 4 K orthorhombic structures with $\langle r_A\rangle = 1.23$ Å. These show that all three displacements increase with σ^2, as these structures are orthorhombic with $\langle r_A\rangle = 1.23$ Å significantly less than $r_A^0 = 1.30$ Å so that the environment around oxygen is less symmetric than in Fig. 1. Nevertheless, it is notable that the mean values of $\Delta u/\sigma^2$ are 0.68 for the O(1) oxygen site and 0.63 for O(2), giving an overall mean of 0.65, in excellent agreement with the predicted $\langle Q^2\rangle/\sigma^2 = 0.67$ value for the increase in mean-squared oxygen displacement with A site disorder. This verifies the use of σ^2 as a functional for displacive disorder of the oxygen atoms due to A site cation size disorder in perovskites.

The increase of u_1 with σ^2 in Figs. 3(b) and 3(c) is particularly significant as it demonstrates an increasing radial distortion resulting in an increasing dispersion in Mn-O bond lengths due to A cation disorder, which can affect the change in u_1 at the metal-insulator transition. Across the series of four samples, the average increase of 0.004 Å^2 in u_1 is equal to the extrapolated $T=0$ difference in u_1 between the metallic and insulating states of $(\mathrm{La_{0.70}Ca_{0.11}Sr_{0.19}})\mathrm{MnO_3}$ estimated above.

A simultaneous electronic (metal to insulator), magnetic (ferromagnetic to paramagnetic), and structural (dynamic to static Jahn-Teller distortions) second-order phase transition occurs in these $A\mathrm{MnO_3}$ perovskites at T_m. Variations in T_m due to lattice effects at a fixed doping level have been ascribed to changes in the double exchange interaction through reduction of the bandwidth. However, the changes in bandwidth are very small, for example, an estimated 3% change was found for a series of $(L_{0.7}M_{0.3})\mathrm{MnO_3}$ samples in which T_m ranges from 350 to 100 K.[8] Bandwidth is calculated from average bond distances and angles, but it is clear that the small changes in average structure at T_m or as a function of changing σ^2 result from much larger changes in disordered structure, which provide an alternative explanation for the strong lattice dependence of T_m through changes in the structural contribution to the energy for polaron localization. The above results show that the large linear decrease in T_m across the series of four samples with increasing σ^2 is accompanied by a large, approximately linear increase in the radial distortions (u_1) of the $\mathrm{MnO_6}$ octahedra. Although u_1 is averaged over many deformations, it will contain components of the Jahn-Teller active orthorhombic and tetragonal distortions[9] which lower the energy for polaron trapping at T_m.

A full treatment of the competition between dynamic and static displacements is beyond the scope of this study, but we note that the linear dependence of T_m upon σ^2, is rationalized by a strain term which may describe the reduction in polaron localization energy at the transition:

$$T_m \approx T_m^0 - \frac{\Sigma K\langle Q_J^2\rangle}{2\Delta S_m}, \tag{1}$$

where the mean square static oxygen displacements of Jahn-Teller symmetry due to A cation disorder $\langle Q_J^2\rangle$ are summed over the all the Jahn-Teller modes, T_m^0 is the transition temperature at $\sigma^2=0$, and ΔS_m is the transition entropy. This enables $dT_m/d\sigma^2$ to be estimated as $dT_m/d\sigma^2 \approx -3K\langle Q_J^2\rangle/\Delta S_m$ for the summation over six Mn-O bonds per Mn cation. Approximating ΔS_m by the dominant magnetic entropy change $\Delta S_m \approx k_B \ln(2\langle S\rangle+1) \approx 1.5k_B$ for $\langle S\rangle = 1.85$ and taking $\langle Q_J^2\rangle/\sigma^2 = \Delta u_1/\sigma^2 = 0.4$ from Figs. 3(b) and 3(c) and $K \approx 100\ \mathrm{Nm^{-1}}$ as before gives $dT_m/d\sigma^2 \approx -60\,000\ \mathrm{K\,Å^{-2}}$. This compares well with the observed value of $-20\,600\ \mathrm{K\,Å^{-2}}$ given the uncertain values of the above parameters and the assumption that all the radial displacements induced by A site disorder are Jahn-Teller active (i.e., that $\langle Q_J^2\rangle = \Delta u_1$), which overestimates the magnitude of $dT_m/d\sigma^2$.

The analogous effects of increasing σ^2 and $(r_A^0 - \langle r_A\rangle)$ in Fig. 1 suggests that decreasing $\langle r_A\rangle$ should also lead to increasing distortions of the $\mathrm{MnO_6}$ octahedra. Evidence for this is contained in the study by Radaelli *et al.* who carried out low-temperature neutron structure refinements on a series of $L_{0.7}M_{0.3}\mathrm{MnO_3}$ compounds with widely varying $\langle r_A\rangle$ and variable σ^2.[8] They found an inverse correlation between T_m and the mean Mn-O distance which, as observed in Fig. 3(a), is a measure of the degree of radial distortion of the $\mathrm{MnO_6}$ octahedra. It has recently been shown that the superconducting critical temperature (T_c) in $L_{1.85}M_{0.15}\mathrm{CuO_4}$ superconductors also decreases linearly with σ^2,[15] demonstrating a general sensitivity of electronic transitions in perovskite-like transition metal oxides to this lattice effect. The large quadratic dependence upon atomic displacements suggests that changing strain contributions to the transition enthalpy are responsible for variations in T_m or T_c at a constant doping level through equations such as Eq. (1). Furthermore changes of transition temperature through changing hole doping by chemical substitutions (e.g., changing x in $\mathrm{La_{1-x}Sr_xMnO_3}$ or $\mathrm{La_{2-x}Sr_xCuO_4}$) reflect both changing lattice and electronic effects, so that maximum transition temperatures do not necessarily coincide with electronically optimum hole doping levels.

The authors acknowledge EPSRC for the provision of neutron facilities and the Basque Government for support for L.M.R.-M.

[1] C. N. R. Rao and A. K. Cheetham, Adv. Mater. **9**, 1009 (1997).
[2] Y. Tokura, Y. Tomioka, H. Kuwahara, A. Asamitsu, Y. Moritomo, and M. Kasai, J. Appl. Phys. **79**, 5288 (1996).
[3] L. M. Rodriguez-Martinez and J. P. Attfield, Phys. Rev. B **54**, R15 622 (1996).
[4] *A* cation radii for ninefold coordination in oxides were taken from R. D. Shannon, Acta Crystallogr., Sect. A: Cryst. Phys., Diffr., Theor. Gen. Crystallogr. **32**, 751 (1976).
[5] Profiles were fitted using the GSAS package, see A. C. Larson and R. B. Von Dreele (unpublished).
[6] P. G. Radaelli, M. Marezio, H. Y. Hwang, and S.-W. Cheong, J. Solid State Chem. **122**, 444 (1996).
[7] P. G. Radaelli, M. Marezio, H. Y. Hwang, S.-W. Cheong, and B. Batlogg, Phys. Rev. B **54**, 8992 (1996).
[8] P. G. Radaelli, G. Iannone, M. Marezio, H. Y. Hwang, S-W. Cheong, J. D. Jorgensen, and D. N. Argyriou, Phys. Rev. B **56**, 8265 (1997).
[9] J. L. Garcia-Munoz, M. Suaaidi, J. Fontcuberta, and J. Rodriguez-Carvajal, Phys. Rev. B **55**, 34 (1997).
[10] P. G. Radaelli, D. E. Cox, M. Marezio, S-W. Cheong, P. E. Schiffer, and A. P. Ramirez, Phys. Rev. Lett. **75**, 4488 (1995).
[11] M. R. Ibarra, J. M. De Teresa, J. Blasco, P. A. Algarabel, C. Marquina, J. Garcia, J. Stankiewicz, and C. Ritter, Phys. Rev. B **56**, 8252 (1997).
[12] D. Louca, T. Egami, E. L. Brosha, H. Roder, and A. R. Bishop, Phys. Rev. B **56**, R8475 (1997).
[13] P. Norby, I. G. Krogh Andersen, E. Krogh Andersen, and N. H. Andersen, J. Solid State Chem. **119**, 191 (1995).
[14] *K* has been estimated to be 30–300 Nm^{-1} by A. J. Millis, Phys. Rev. B **53**, 8434 (1996).
[15] J. P. Attfield, A. L. Kharlanov, and J. A. McAllister, Nature (to be published).